Ceramics International 48 (2022) 12132–12141

Contents lists available at ScienceDirect

Ceramics International

journal homepage: www.elsevier.com/locate/ceramint

The best diffusivity proxy for crystal nucleation in stoichiometric oxide glasses

María Helena Ramírez Acosta, Lorena Raphael Rodrigues *, Edgar Dutra Zanotto

Federal University of São Carlos, Graduate Program in Materials Science and Engineering, Department of Materials Engineering, São Carlos, SP, Brazil

ARTICLE INFO

Keywords:
Diffusivity
Nucleation
Crystal growth
Viscosity
Glass

ABSTRACT

Due to the difficulty in measuring the mobility of the "structural units" of supercooled liquids and glasses during crystal nucleation, the effective diffusivity (D) has been frequently estimated via viscosity (D_η) or nucleation time-lags (D_τ). However, it has been recently reported that, below the glass transition temperature (T_g), the experimental steady-state nucleation rates (I_{st}) can reach much *higher* values than those predicted by the Classical Nucleation Theory (CNT) when assuming $D \approx D_\eta$ or $D \approx D_\tau$. Hence, another possibility would be inferring D from experimental crystal growth velocity data ($D \approx D_U$), which is a natural approach since nucleation and growth are likely controlled by the same mass transfer process through the crystal/liquid interface. Therefore, the approximations $D \approx D_\eta$ and $D \approx D_U$ were tested in this work using lithium disilicate glass as a model system. To avoid the influence of compositional changes, we measured the nucleation rates, growth velocity, and viscosity using samples of the *same* glass batch. With this strategy, we found that the very long experimental nucleation times implemented below T_g shifted the experimental temperature of maximum nucleation rate to temperatures lower than those previously reported for this glass former. Most important is that the CNT gives a much better description of the experimental $I_{st}(T)$ data in the whole analyzed temperature range if D is approximated by D_U instead of D_η, indicating that crystal growth is indeed an adequate proxy for nucleation diffusivity.

1. Introduction

Knowledge about the effective diffusion coefficient controlling crystal nucleation (D) is a critical factor in understanding, evaluating, or predicting nucleation kinetics by any nucleation theory. However, due to the difficulty in defining the "structural units" and measuring D, especially in multielement glass-forming systems, the most adequate property to evaluate the kinetic barrier in the framework of the classical nucleation theory (CNT) is still a matter of strong debate.

One alternative to estimate D is via nucleation time-lags (τ) [1,2], since τ is directly related to the kinetics of the nucleation process. However, there are many uncertainties in the definition and measurement of the actual values of this parameter and, consequently, of the corresponding diffusion coefficient (D_τ). Due to the distorting effect of double-stage heat treatments commonly used in nucleation experiments, the experimental values of τ, which are supposedly dependent only on the chemical composition and nucleation temperature, are also affected by the experimental conditions of the second-stage heat treatment [3]. According to Ref. [3], τ is affected by the heating rate (q_2) between the nucleation and the development heat treatments due to the temperature dependence of the critical nucleus size. Thus, to prevent the dissolution of a significant fraction of supercritical clusters during the development stage, q_2 should be small enough to allow their growth up to the new critical size during the heating path between nucleation and development temperatures. For this reason, a direct comparison of the values of τ obtained in different works requires knowledge of the q_2 used, even when the same glass composition and temperatures are used. In addition, at temperatures above T_g, the induction times for nucleation are too short, hindering their accurate determination through the experimental nucleation data. Another drawback in using D_τ as a proxy for the kinetic barrier is the strong effect of the relaxation process on nucleation dynamics at low temperatures, below T_g [4–6], exactly when transient nucleation is detectable. Despite this problem, we did not consider the relaxation effect on nucleation because we are not interested in D_τ for the particular problem under analysis. Besides, as we will show later, the current nucleation rate data were obtained using very long nucleation treatments, and in such case, it is most likely that the system had already completed its relaxation process. Due to all these potential problems, the

* Corresponding author.
E-mail address: lorena.raphael92@gmail.com (L.R. Rodrigues).

https://doi.org/10.1016/j.ceramint.2022.01.074
Received 9 November 2021; Received in revised form 4 January 2022; Accepted 8 January 2022
Available online 17 January 2022

measurement of the actual values of τ is quite complex and unreliable.

On the other hand, a widespread practice consists in estimating D via the equilibrium viscosity (η) [7,8], since it is relatively straightforward to measure this property independently, avoiding the problems associated with the determination of τ. Even though the approximation $D \approx D_\eta$ is an adequate option from a practical point of view, viscous flow is a cooperative bulk process, whereas nucleation dynamics is governed by local atomic or molecular transfer though the crystal/liquid interface. Owing to this conceptual difference between these two properties, it is expected that D_τ leads to a more accurate approximation of D than D_η. However, there are contradictory results in the literature regarding these coefficients, making it difficult to discern which is the best. Although some authors [9,10] have shown a divergence between D_τ and D_η, at least in Ref. [11] it was suggested that both coefficients present a similar temperature dependence in the range of measurable nucleation rates. However, the limitations to obtain precise values of τ from experimental transient nucleation data makes η a much more accessible and reliable parameter to estimate diffusivity, which is the reason of its common use.

Alternatively, D could be inferred via crystal growth velocities (D_U), as scarcely reported for metallic [12] and organic glasses [13], and recently proposed in Refs. [4,6] for silicate glasses. From a theoretical point of view, the hardly applied assumption $D \approx D_U$ is supported by the fact that the nucleation and growth processes in stoichiometric glass forming systems are, in principle, controlled by the same atomic or molecular transfer mechanism trough the crystal/liquid interface [9,14]. In this regard, recent experimental results [4] for $Li_2O{\cdot}2SiO_2$ glass have shown that the steady-state nucleation rates (I_{st}) below T_g can reach values much *higher* than those predicted by the CNT assuming $D \approx D_\eta$, and tend to approach the values predicted by the CNT considering $D \approx D_U$. Additionally, a comparative analysis performed in Ref. [6] indicates that D_U gives a better description of the isothermal time dependence of the crystal number density in $2Na_2O{\cdot}CaO{\cdot}3SiO_2$ glass at any temperature below T_g.

In this respect, molecular dynamics (MD) simulations of simple liquid models, such as Lennard-Jones, BaS, Ge and ZnSe [15–18], have shown that the atomic self-diffusion coefficients describe well mass transfer through the crystal-liquid interface during nucleation. It is worth mentioning that these diffusion coefficients were obtained directly from the simulations with no approximations and fitting procedures. For complex glass-formers, such as multicomponent oxide systems, direct determinations of D through experiments or MD simulations are highly recommended to finally solve this issue; however, the lack of knowledge about the nature of the "structural units" in these complex systems and the slow dynamics (from a MD simulation perspective) have so far precluded such determinations.

To shed light on this central topic in glass science, in the present work we will test, in detail, two approximations for D ($D \approx D_\eta$ and $D \approx D_U$) in the CNT framework using a lithium disilicate glass (LS_2) as a model system. For the sake of completeness, the coefficient D_τ (despite its several aforementioned complications) will also be determined and compared with D_η and D_U.

2. Materials and methods

For this study, a lithium disilicate glass ($Li_2O{\cdot}2SiO_2$ - LS_2) was chosen as a model system, since this composition presents internal homogeneous nucleation rates that are measurable in laboratory time scales. Moreover, its adequate (neither very low, nor extremely high) experimental maximum nucleation rate ($I_{max} \sim 10^9$ $s^{-1}m^{-3}$) [19,20] allows measurement of the crystal number density (N_v) in a wide temperature range, above and below the glass transition temperature (T_g), for considerably long nucleation times without presenting crystal impingement. Additionally, this system permits the measurement of crystal growth velocities and viscosity in similar temperature ranges.

The LS_2 glass used here was prepared in a previous work [3], following the conventional repeated melting/crushing/remelting and splat cooling process. To mitigate incipient nucleation, no annealing treatment was performed. The procedures used to determine its chemical composition ($32.81Li_2O{\bullet}67.19SiO_2$ mol%), and glass transition temperature (~ 728 K) inferred from a DSC heating curve, can be consulted in Refs. [3,20], respectively.

Table 1
Temperatures (T_n and T_d) and times (t_n and t_d) used in the nucleation experiments in the current work.

T_n (K)	t_n (h)	T_d (K)	t_d (min)
708	15–792	865	1.3–15
715	28–384		1.5–8
723	48–168		2–7
768	2–16		9–17

Crystal growth velocities were measured in samples of the same glass batch used for the nucleation and viscosity measurements in Ref. [20] at several temperatures: T_U = 708, 743, 763, 773, 865, 875, and 885 K. Since only a few nuclei are present in the as-quenched samples because of the small overlap between the $I(T)$ and $U(T)$ curves, the isothermal heat-treatments at T_U = 773–885 K were preceded by a nucleation treatment at 753 K for 2 h. On the other hand, at the three lowest T_U we performed single-stage heat treatments to measure $U(T)$, because, in this case, the overlap between the nucleation and growth curves is considerable.

The $U(T)$ dependence was evaluated from the linear fit of the largest dimension of the largest crystal observed in optical micrographs as a function of time (R(t)). The error in U at each T_U corresponds to the error from the linear fit of the R(t) experimental data. For the sake of comparison, experimental data of the LS_2 crystal growth velocities at a wide range of temperatures (T_U) were obtained from the literature [21–24]. Thus, the temperature range comprising all the measured and literature $U(T)$ data ranges from 708 to 913 K, i.e., including temperatures below $1.1T_g$, where the well-known decoupling between the diffusion coefficient estimated from viscous flow and crystal growth occurs [25], allowing us to make a reliable extrapolation of the $U(T)$ data down to nucleation temperatures below T_g.

To obtain the $N_v(t)$ plots, double-stage heat treatments were implemented. The first stage consisted in keeping some samples at a selected nucleation temperature (T_n) for increasing nucleation times (t_n),

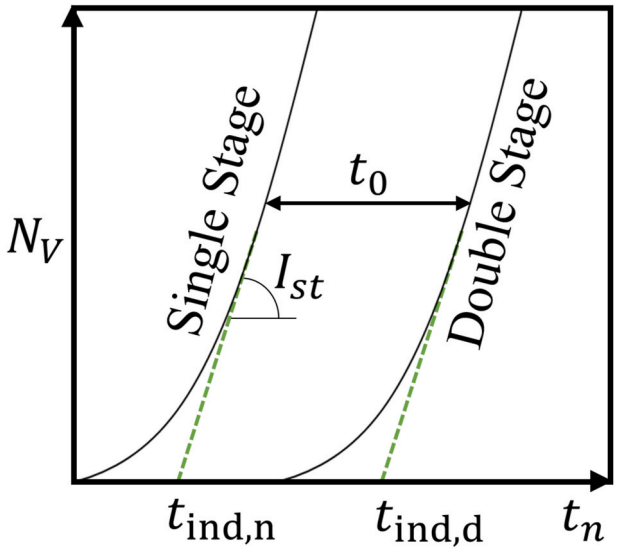

Fig. 1. Time dependence of the crystal number density for single and double stage heat treatments. The heat treatment at T_d creates a shift t_0 in the single stage curve.

followed by a second heat treatment, in which the samples were submitted to a development temperature (T_d) for a certain time (t_d) to promote growth of the critical nuclei up to observable sizes [26]. The temperatures T_n and T_d were chosen based on literature data for LS_2 glass to warrant that $I(T_d) \ll I(T_n)$ and $U(T_d) \gg U(T_n)$. Some experimental $N_v(t)$ curves for samples of the current glass batch were already presented in Ref. [20] for T_n = 715, 723, 733, 745, and 753 K at a maximum t_n = 54, 48, 20, 19 and 26 h, respectively. To check this work's hypothesis, we collected nucleation rate data at T_n = 708 and 768 K, two different temperatures from those analyzed in Ref. [20]. Additionally, the treatment times, t_n, used in Ref. [20] at T_n = 715K and 723 K were significantly extended. The treatment temperatures and times are shown in Table 1. Uncertainties in $N_v(t)$ data were determined via error propagation.

Both nucleation and growth heat treatments were performed in vertical furnaces with a precision of ±1 K using samples of ~4 × 4 × 3 mm^3. After the heat treatments, the samples were ground using SiC sandpaper of progressively finer grits (400–1200), polished with a CeO_2 suspension with an average particle size of ~3 μm, and finally submitted to an ultrasound bath in water at a frequency of 37 kHz for 10 min to reveal the crystals. Posteriorly, the cross-sections of the samples were observed by reflected light optical microscopy (Leica DMRX and Nikon Eclipse LV100 N POL) to determine the average number of crystals per unit area ($\overline{N}_s$) and the size of the largest crystals. To obtain N_v, we used the equation proposed by De-Hoff and Rhines [27], according to which:

$$N_v^m = \frac{2}{\pi K(q)} \overline{N}_s \overline{z}, \tag{1}$$

where N_v^m is the measured crystal number density, $\overline{z}$ is the average of the reciprocal of the minor axis of the largest crystal traces detected in the micrograph, and K(q) is a function of the aspect ratio of the largest crystals (q). Since LS_2 presents prolate ellipsoidal crystals, K(q) ≠ 1, and in this case the following equation applies [27]:

$$K(q) = \frac{1}{q} + \frac{q \ \ln\left[\left(1+\sqrt{1-q^2}\right)/q\right]}{\sqrt{1-q^2}}. \tag{2}$$

Due to the resolution limit of the optical microscopes (ε ~ 0.3–0.7 μm, depending on the microscope objective), a fraction (f) of the actual number of crystals in the cross-section may be underestimated. To avoid this problem arising from the stereological method, the following correction [28] was used:

$$f = \frac{2}{\pi} \sin^{-1} \frac{\varepsilon}{D_M}, \tag{3}$$

$$N_v = \frac{N_v^m}{1-f}. \tag{4}$$

In Eqs. (3) and (4), D_M is the dimension of the largest crystal in the cross-section and N_v is the corrected value of crystal number density. Eq. (3) was derived assuming that the crystals present a monodisperse distribution [8,28], which is a reasonable hypothesis due the double-stage method used in the nucleation experiments, since this method favors an uniform growth and size of all the super critical nuclei. The experimental values of I_{st} were obtained by fitting the $N_v(t)$ data with Eq. (5) proposed by Kashchiev [29].

$$N_v(t) = I_{st}\tau\left[\frac{t-t_0}{\tau} - \frac{\pi^2}{6} - 2\sum_{n=1}^{\infty}\frac{[-1]^n}{n^2}\exp\left(-n^2\frac{t-t_0}{\tau}\right)\right], \tag{5}$$

where τ represents the nucleation time-lag and t_0 is the time shift on the $N_v(t)$ curve resulting from the double-stage heat treatment (Fig. 1).

In the original and modified formulation of the Kashchiev equation, the parameters τ and t_0 are related through $\tau_n = \frac{6}{\pi^2} t_{ind,n}$ and $\tau_n = \frac{6}{\pi^2}(t_{ind,d} - t_0)$, for the case of a single and a double-stage experiments, respectively. Both times, $t_{ind,\ n}$ and $t_{ind,\ d}$ are illustrated in Fig. 1. The magnitude of t_0 is mainly dependent on T_d and q_2 between T_n and T_d [3]. In this work, q_2 was estimated as ~910 $Kmin^{-1}$. Taking this value into account, it is possible to carry out a proper comparison between the τ values reported in this work and in other references. In Eq. (5), I_{st}, t_0 and τ are used as fitting parameters and their errors were obtained from the fit. Since it was not possible to obtain reliable values for t_0 in the non-linear regression of the $N_v(t)$ data, this parameter was assumed to be zero. As illustrated in Fig. 1, for the case of a double-stage experiment, this approximation can affect the values of τ due to its interdependence with t_0 and $t_{ind,\ d}$. Nevertheless, I_{st} is not affected provided the nucleation treatment is long enough [3], which is indeed the case in this work. Therefore, since I_{st} is the main parameter considered in our analysis, the approximation $t_0 = 0$ does not influence our conclusions.

Since the LS_2 glass samples used here and in Ref. [20] were from the same batch, the temperature dependence of the equilibrium viscosity η(T) (Eq. (6)) was taken from Ref. [20], using the MYEGA model [30]:

$$\log_{10}(\eta(T)) = \log_{10}(\eta_\infty) + \frac{T_{12}}{T}[12 - \log_{10}(\eta_\infty)]\exp\left(\left[\frac{m}{12-\log_{10}(\eta_\infty)} - 1\right]\left[\frac{T_{12}}{T} - 1\right]\right), \tag{6}$$

where $T_{12} = (734.5 \pm 0.4)$ K, $m = 43 \pm 1$, and $\log_{10}(\eta_\infty) = (-7 \pm 9)$ Pa.s. The large uncertainty in the fitting parameter $\log_{10}\eta_\infty$ is due to the lack of viscosity data at high temperatures, around T_{max}. The uncertainties in the parameters of Eq. (6) were obtained from the fit of the η(T) experimental data [20].

3. Governing equations

The steady-state nucleation rate (I_{st}) is proportional to the probability that a structural fluctuation in the metastable supercooled-liquid (SCL) results in the formation of a larger nucleus than the critical size imposed by the thermodynamic barrier [31]. Assuming the formation of spherical and isotropic nuclei in a SCL, the CNT predicts the temperature dependence of I_{st} according to Refs. [8,32–34]:

$$I_{st}(T) = \frac{D}{d_0^4}\sqrt{\frac{\sigma}{k_B T}}\exp\left(-\frac{16\pi\sigma^3}{3k_B T \Delta G_v^2}\right), \tag{7}$$

where D is the effective diffusion coefficient for crystal nucleation, k_B is Boltzmann's constant, σ is the surface energy of the critical nucleus/SCL interface, ΔG_v is the thermodynamic driving force for crystallization per unit volume, and d_0 is the average size of the structural units, which has the order of magnitude of the crystal lattice parameter and is commonly calculated as $d_0 \approx \sqrt[3]{V_m/N_A}$, where V_m is the molar volume and N_A the Avogadro's number. For LS_2, $d_0 = 4.67 \times 10^{-10}$ m, considering $V_m = 61.2 \times 10^{-6}$ m^3mol^{-1} [26].

For a reasonable estimate of $\Delta G_v(T)$, we considered the polynomial dependence given in Eq. (8), which was calculated from the experimental data of Takahashi and Yoshio for the LS_2 system [35]:

Table 2
Parameters *a*, *b*, *q*, and *p* in Eq. (16), assuming $D \approx D_\eta$ and $D \approx D_U$, from Eqs. (10) and (14), respectively.

Equation	*a*	*p*	*b*	*q*
(10)	$\sqrt{k_B T}(I_{st}\eta d_0^5)^{-1}$	1/2	$-\frac{16\pi}{3\Delta G_V^2 k_B T}$	3
(14)	$8\pi T_m U[I_{st}(T_m - T)d_0^3\sqrt{k_B T}]^{-1}$			

$$\Delta G_V(T) = 8.40245028 \times 10^8 - 540266\,T - 78.5116\,T^2, \tag{8}$$

with ΔG_V in Jm^{-3} and T in K. A widely used estimate of *D* for nucleation in SCLs is the diffusion coefficient for viscous flow (D_η), which can be calculated through the Stokes-Einstein-Eyring relation [36,37]:

$$D_\eta(T) = \frac{k_B T}{d_0 \eta(T)}. \tag{9}$$

With Eq. (9), Eq. (7) becomes:

$$I_{st}\left(T\right) = \frac{\sqrt{\sigma_\eta(T) k_B T}}{d_0^5 \eta(T)} \exp\left(-\frac{16\pi\sigma_\eta^3(T)}{3k_B \Delta G_V^2(T)}\right). \tag{10}$$

A much less common alternative is to estimate *D* from crystal growth velocities (D_U) [4,6,12,13]. Considering the screw dislocation mechanism–the most common for crystal growth in silicate glasses–D_U can be described by Eq. (11) [9], in which the thermodynamic term given by $1/[1-\exp(-\Delta G_v d_0^3/k_B T)]$ was neglected since at the analyzed temperature range it is ~1. Therefore, at deep supercoolings where homogenous nucleation is experimentally detected, the crystal growth velocity is mainly governed by the kinetic factor shown in Eq. (11):

$$D_U(T) = \frac{8\pi T_m d_0 U(T)}{T_m - T}, \tag{11}$$

where T_m is the melting temperature and $U(T)$ is the temperature-dependent growth velocity. In the temperature range of measurable homogeneous nucleation rates, below the temperature of the Stokes-Einstein-Eyring relation breakdown, $U(T)$ presents an Arrhenian behavior:

$$U(T) = U_0 \exp\left(-\frac{E_U}{k_B T}\right), \tag{12}$$

where U_0 is a pre-exponential term and E_U is the activation energy for crystal growth. With this expression for $U(T)$, Eq. (11) can be rewritten as:

$$D_U(T) = \frac{8\pi T_m d_0}{T_m - T} U_0 \exp\left(-\frac{E_U}{k_B T}\right). \tag{13}$$

Hence, substituting Eq. (13) in Eq. (7), it follows that:

$$I_{st}(T) = \frac{8\pi T_m}{T_m - T}\frac{U_0}{d_0^3}\exp\left(-\frac{E_U}{k_B T}\right)\sqrt{\frac{\sigma_U(T)}{k_B T}}\exp\left(-\frac{16\pi\sigma_U^3(T)}{3k_B \Delta G_V^2(T)}\right). \tag{14}$$

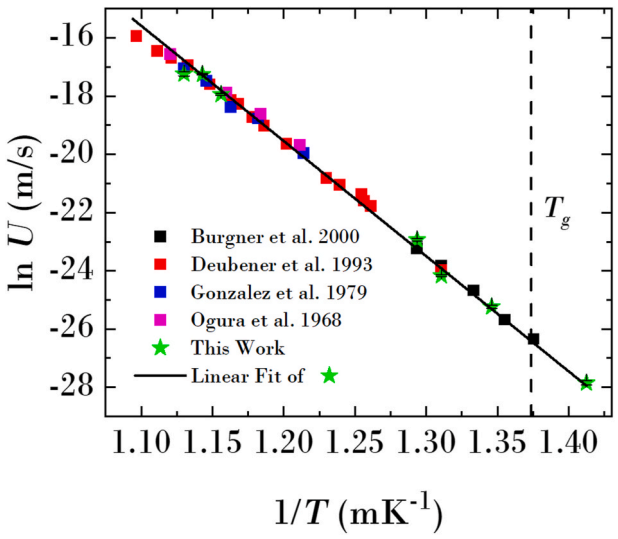

Fig. 3. Temperature dependence of crystal growth rates for the LS2 glass comparing literature data (colored squares) with those from this work (green stars). The black line denotes the fit of Eq. (12) to the U(T) data of this work. The error bars' size is smaller than the symbols. (For interpretation of the references to color in this figure legend, the reader is referred to the Web version of this article.)

Another alternative to determine *D* is through the diffusion coefficient from nucleation time-lags (D_τ), which is given by Ref. [1]:

$$D_\tau(T) = \frac{16}{3}\frac{k_B T \sigma}{\Delta G_v^2(T) d_0^2 \tau(T)}. \tag{15}$$

In Eq. (15), σ was considered equal to the interfacial energy of a planar interface (σ_∞), which was calculated trough the macroscopic approximation of this parameter given by the Turnbull-Skapski equation: $\sigma_\infty = \alpha \Delta H_m / \sqrt[3]{N_A V_m^2}$, where ΔH_m is the molar melting enthalpy and α a non-dimensional parameter between 0.4 and 0.5 for homogeneous nucleation in oxide SCLs. With $\Delta H_m = 61086.4\ Jmol^{-1}$ [35] and $\alpha = 0.44$ [38], this approximation leads to $\sigma = 0.205\ Jm^{-2}$. As shown by Eqs. (4) and (8), the interfacial energy is an important parameter in the CNT. As a consequence of the diffuse character of the crystal/SCL interface and of the atomic order that is gradually established in the SCL near the evolving crystal clusters [39], σ is expected to have a positive temperature dependence. The subscripts η and *U* for σ in Eqs. (10) and (14) refer to the fact that these are fitted interfacial energies resulting from using D_η and D_U, respectively, as proxies for *D*. The temperature dependences of σ_η and σ_U were calculated through the numerical solution proposed in Ref. [40], according to which:

$$\sigma = \left[\frac{p}{bq} W_n\left(\frac{bq}{p} a^{-\frac{q}{p}}\right)\right]^{\frac{1}{q}}, \tag{16}$$

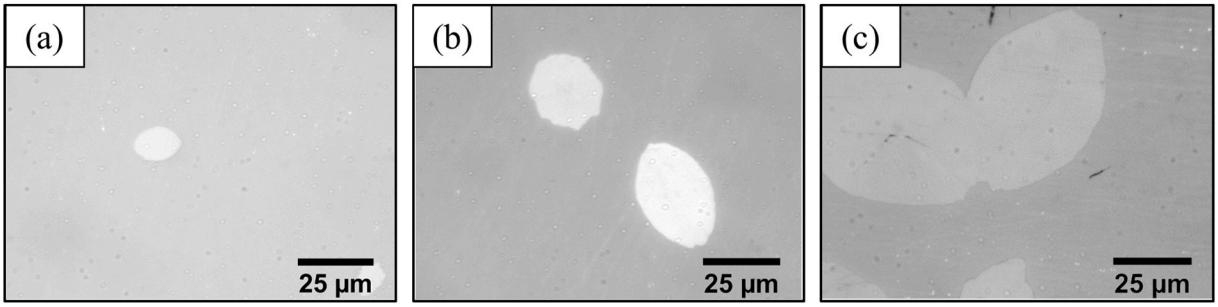

Fig. 2. Reflected light optical micrographs of the LS_2 glass treated at T_n = 753 K for 2 h, and at T_U = 875 K for (a) 5, (b) 10, and (c) 20 min.

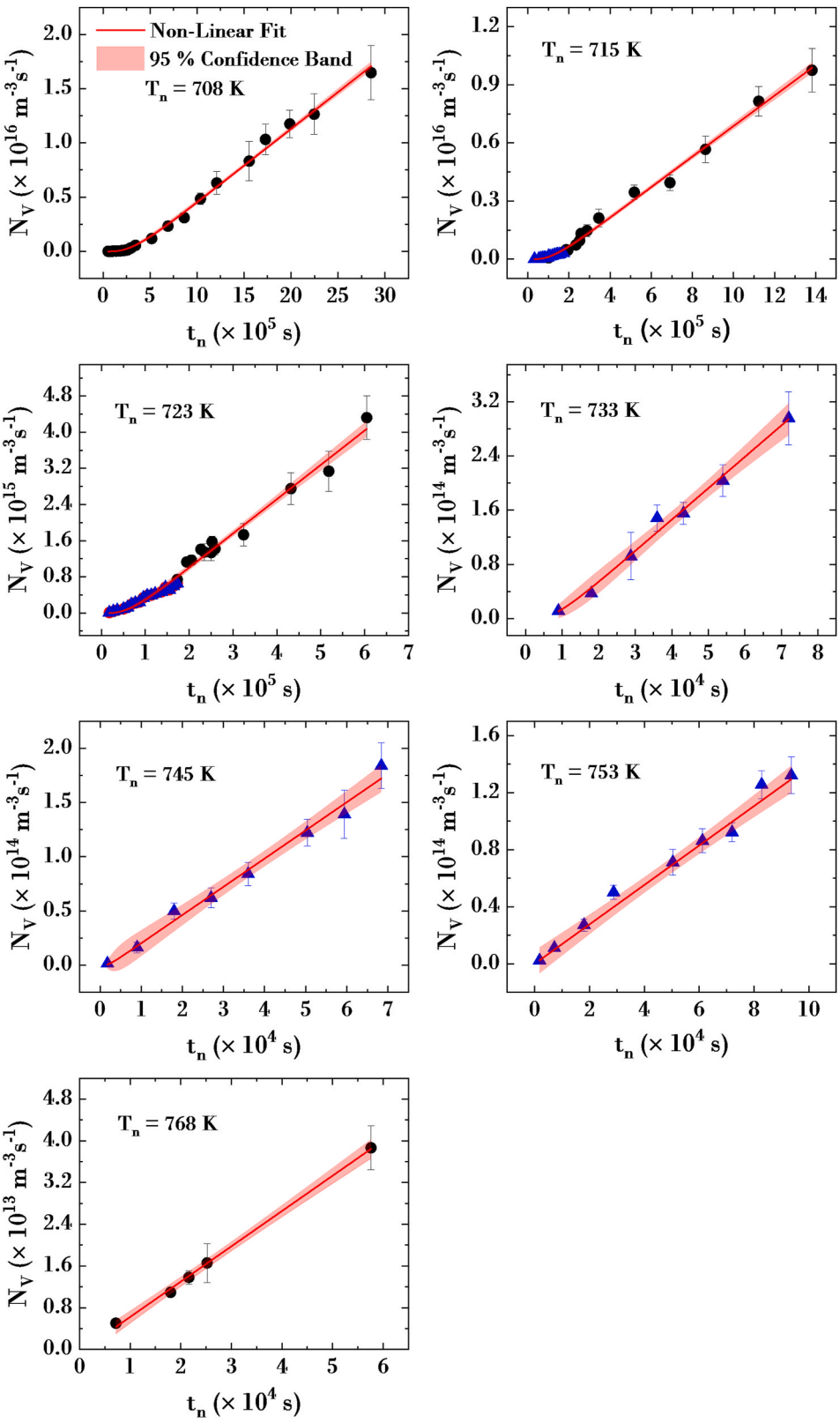

Fig. 4. Time dependence of the number of crystals per unit volume (N_v) for T_n = 708–768 K. The blue triangles represent the experimental data from Ref. [20] and the black dots refer to data of this work. The red lines correspond to a non-linear fit of Eq. (5) to the experimental data, and the shaded area indicates the 95% confidence band. (For interpretation of the references to color in this figure legend, the reader is referred to the Web version of this article.)

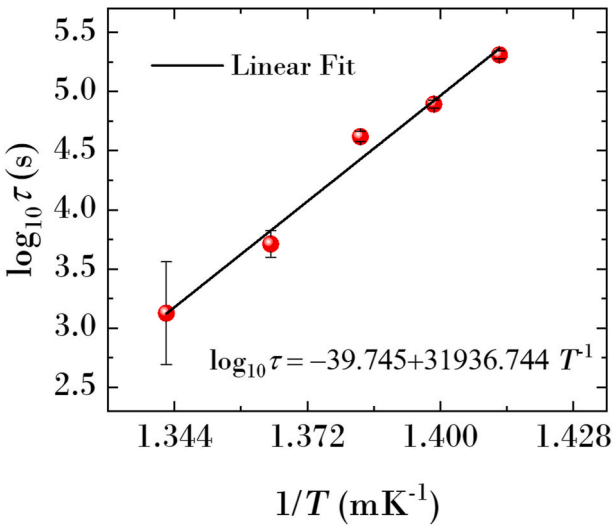

Fig. 5. Temperature dependence of the nucleation time-lags (τ). The values of τ were obtained through a non-linear fit of Eq. (5) to the experimental $N_v(t)$ data.

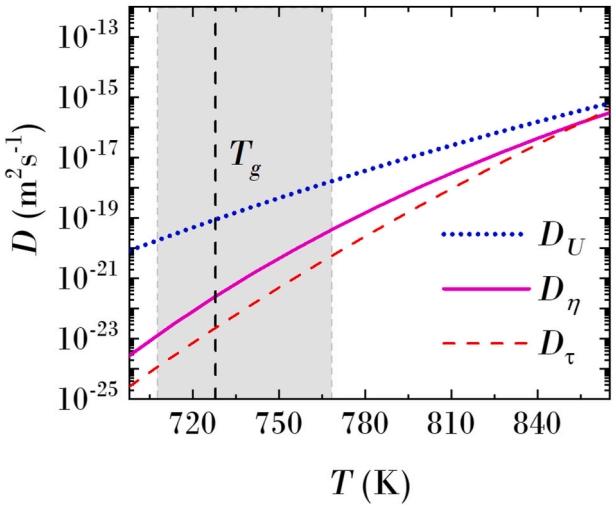

Fig. 6. Diffusion coefficients calculated from the equilibrium viscosity (magenta solid line), crystal growth velocities (blue dotted line), and nucleation time-lags (red dashed line) for the LS_2 system, by using Eqs. (9), (13) and (15), respectively. The temperature range where I_{st} was measured is delimitated by the shaded area, and T_g is indicated by the vertical dashed line. (For interpretation of the references to color in this figure legend, the reader is referred to the Web version of this article.)

where W_n is the multivalued Lambert function and n represents the branch point, where it takes a single value. Since real results of W_n are only obtained for $n = -1$ and $n = 0$, for values of σ with physical meaning, we solved the Lambert function for $n = -1$. The parameters a, b, q, and p in Eq. (16) are dependent on the CNT formulation, as summarized in Table 2 for Eqs. (10) and (14). The error propagation in σ was computed using the Python uncertainties module [41].

4. Results

4.1. Crystal growth

Fig. 2 shows some representative optical micrographs at $T_U = 875$ K for increasing t_U, used for the $U(T)$ determination.

Fig. 3 shows a comparison between the experimental crystal growth rate data from the literature [21–24] and those from this work for LS_2,

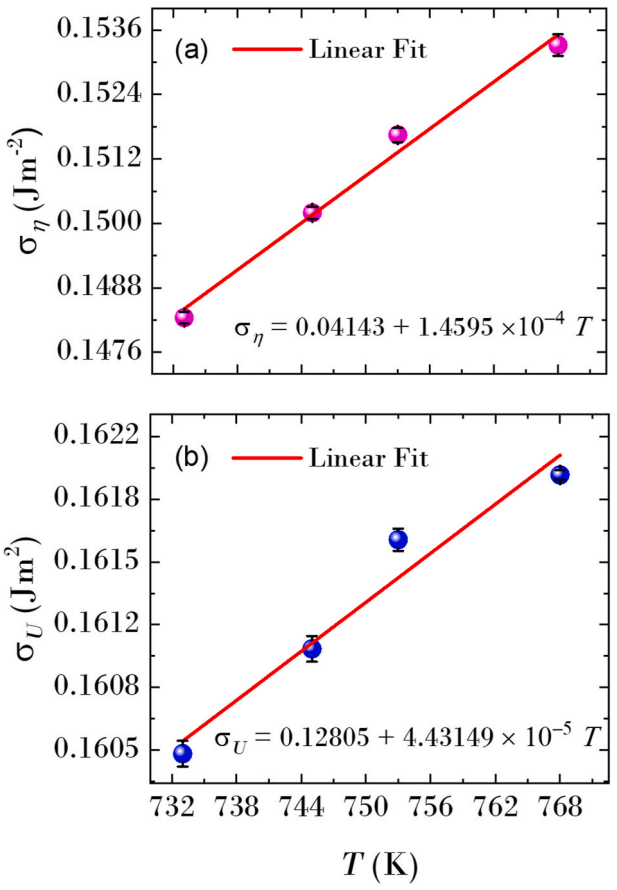

Fig. 7. Temperature dependence of σ considering (a) $D \approx D_\eta$ and (b) $D \approx D_U$. The linear fitting procedure was performed considering only the I_{st} data above the T_{max} reported in Ref. [20].

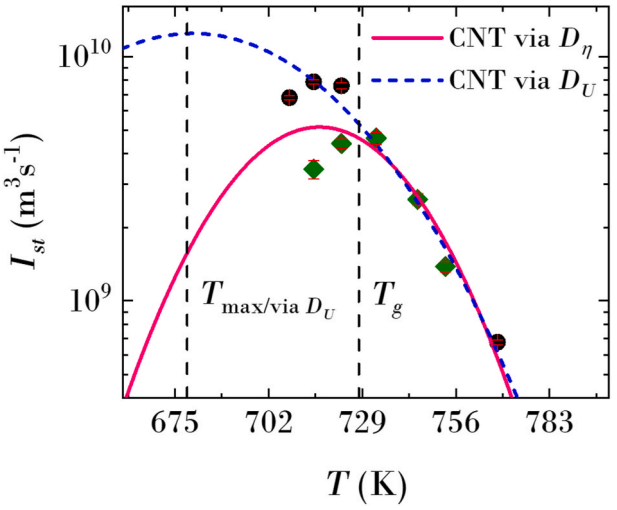

Fig. 8. Temperature dependence of crystal nucleation rates in the LS_2 system in logarithmic scale. The blue dashed line and the magenta solid line denote the CNT prediction using D_U and D_η as diffusivity proxies, respectively. The green rhombuses correspond to the data of [20], and the black dots represents the data of this work using longer treatment times. The vertical dashed lines indicate T_g and the T_{max} predicted by assuming $D \approx D_U$. The error bars' size is smaller than the symbols. (For interpretation of the references to color in this figure legend, the reader is referred to the Web version of this article.)

indicating the Arrhenian behavior of $U(T)$, with characteristic values of $U_0 = 1.34\times10^{12}$ ms^{-1} and $E_U = 5.46\times10^{-19}$ J (Eq. (12)).

For a "clean" analysis, the linear regression of the data in Fig. 3 was performed using only the data of this work.

4.2. Crystal nucleation

Fig. 4 shows the time dependence of N_v obtained by combining the experimental data from Ref. [20] with those of this work for samples of the *same* batch. The solid lines show the fit of Eq. (5) to the experimental data. The N_v experimental data of LS_2 glass is available in the Supplementary material.

For the highest nucleation temperatures, it was not possible to infer the values of τ from fitting Eq. (5) to the $N_V(t)$ experimental data, since, in such temperature range, the obtained values for τ were negative or showed an error bigger than τ itself. This result is due to the far too short nucleation induction times (only a few minutes to seconds) at such high temperatures.

4.3. Diffusion mechanism and CNT test

For comparison, the diffusion coefficient calculated from nucleation time-lags (D_τ), Eq. (15), was determined from the fitted values of τ (Fig. 5), whose error comes from the fit of Eq. (5) to the $N_V(t)$ experimental data in Fig. 4.

Due to several difficulties in getting reliable values of τ from the fit of Eq. (5) to the $N_v(t)$ curves at the highest temperatures (Section 4.2), the temperature dependence of τ was determined through a linear fit of the τ values obtained at low temperatures, which presented positive values and a standard deviation lower than τ itself.

Such a fit is presented in Fig. 5, including the lowest nucleation temperatures at which the induction times were measurable. Considering the temperature dependence of viscosity, crystal growth velocity, and nucleation time-lags (Fig. 5), the calculated coefficients D_η (Eq. (9)), D_U (Eq. (13)), and D_τ (Eq. (15)) are compared in Fig. 6.

The I_{st} obtained from fitting Eq. (5) to the $N_v(t)$ curves (Fig. 4) were used to determine the temperature dependence of σ. Fig. 7(a) and (b) show the resulting $\sigma(T)$ estimated for $D \approx D_\eta$ and $D \approx D_U$ (Eq. (16)), respectively, for temperatures higher than the experimental T_{max} reported in Ref. [20].

Fig. 7 does not include $\sigma(T)$ resulting from $D \approx D_\tau$, since the values of τ at the two highest temperatures presented a high standard deviation. Finally, the $I_{st}(T)$ curves are shown in Fig. 8, where the magenta solid line and the blue dashed line were calculated via Eqs. (10) and (14) considering the linear dependencies of $\sigma_\eta(T)$ and $\sigma_U(T)$ presented in Fig. 7.

5. Discussion

As shown in Fig. 3, the measured growth velocities agree with those reported in the literature [21–24] and present an Arrhenius behavior, allowing an accurate determination of $U(T)$ and, consequently, of $D_U(T)$ in the temperature range of the nucleation measurements.

According to Fig. 6, in the low temperature range where the I_{st} were measured, D_U increases as the temperature decreases and can be two orders of magnitude greater than D_η. This difference is expected because of the well-known decoupling between these two coefficients [9,25,42]. As a consequence, as shown in Fig. 8, the use of D_U as a proxy for D leads to higher values for the predicted I_{st} compared with those calculated using $D \approx D_\eta$ (Eq. (10)). Also, in Fig. 6, D_τ and D_η show a similar temperature dependence in the range of nucleation measurements. Therefore, the use of D_τ or D_η in the CNT analysis should provide similar conclusions. Nevertheless, using D_η avoids the uncertainties related to the determination of τ, and for this reason, it is considered more appropriate.

Comparison of the experimental I_{st} of this work with those of our previous study [20] and with the values predicted by the CNT considering $D \approx D_\eta$ and $D \approx D_U$ (Fig. 8) shows that the much longer nucleation times used in the current work lead to a significant increase in the "apparent" I_{st}, exceeding the prediction of the CNT with D_η as a proxy for diffusivity. This phenomenon is also exhibited by the steady-state nucleation rate obtained from the new data at 708 K, which is much higher than that predicted by the CNT for this temperature using $D \approx D_\eta$. This increase in I_{st} agrees with the results recently presented in Refs. [20,43], which demonstrate the absence of the CNT "breakdown" at T_{max} when the steady-state nucleation rates are properly determined.

According to three recent works [4–6], a plausible explanation for the progressive increase in I_{st} at low temperatures is the strong effect of structural relaxation below T_g, which leads to much longer t_n necessary to reach the actual I_{st} in a fully relaxed SCL. The changes in the short-range order of LS_2 glass associated to annealing at temperatures far below T_g observed in Ref. [44] are a direct evidence of such effect, which however requires a more in-depth study.

As shown in Fig. 8, the new data obtained with much longer nucleation times are best described when D is estimated from D_U. This result is a consequence of the prolongation in the nucleation heat treatments below the "supposed" T_{max} reported in Ref. [20] and in several other previous studies on LS_2 glass. Therefore, if only the experimental data from Ref. [20] were used, I_{st} would not reach the curve predicted by the CNT using $D \approx D_U$. Additionally, the experimental T_{max} obtained with the long-time data of this work is shifted to much lower temperatures compared with the previous results for samples of the same glass batch [20]. This result agrees with recent observations made for a $2Na_2O{\cdot}CaO{\cdot}3SiO_2$ ($N_2C_1S_3$) glass [6] and for samples of another LS_2 glass batch [4]. Finally, it is corroborated by an analysis of $BaO{\cdot}2SiO_2$ glass presented in the **Appendix**.

The results of this work give new evidence supporting $U(T)$ as a better parameter to estimate the nucleation process diffusivity, since the prediction of $I_{st}(T)$ assuming $D \approx D_U$ (Eq. (14)) indicates that the actual T_{max} could be ~50 K lower than the value commonly reported for LS_2 glass.

These new experimental results and analyses for the LS_2 and BS_2 systems strongly support the hypothesis that D_U is a more adequate parameter than D_η to describe the effective diffusivity controlling crystal nucleation. This conclusion is grounded on the fact that nucleation and growth are simultaneous processes controlled by atomic jumps at the crystal/SCL interfaces. Moreover, recent molecular dynamics simulations showed that the diffusivity in SCLs at deep supercoolings could be predicted by $U(T)$ [45]. A definitive answer about which parameter best describes D can be obtained through a direct measurement of the mobility of "structural units" during the nucleation process, which in the case of multicomponent systems is currently extremely difficult. Here, atomist simulations could be of great relevance [16–18].

6. Summary and conclusions

We evaluated whether the diffusion coefficients estimated via the equilibrium viscosity, nucleation time-lags, or crystal growth velocities best predict the steady-state nucleation rates in the framework of the classical nucleation theory. To this end, we measured the steady-state nucleation rates of a lithium disilicate glass–used as a model–at temperatures below the glass transition range. For this task, we used extremely very long nucleation times (up to 792 h) at 20 K below T_g and combined the nucleation rates with crystal growth velocities and viscosity measured in samples of the *same* glass batch.

The results for LS_2 glass showed that in isothermal treatments at temperatures below T_g, the nucleation rate continuously increases with the treatment time, yielding higher values than those predicted by the CNT if D_η is used as a diffusivity proxy. Besides confirming that the alleged "breakdown" of the CNT at $T_{max} \sim T_g$ is just a consequence of using underestimated nucleation rate data, this work supports recent experimental evidence that very long thermal treatments below T_g can

reveal the actual temperature of maximum nucleation rates, which is far below the values previously reported for LS_2. Similar results were obtained with a barium silicate glass (presented in the **Appendix**).

The most important result of this work is that it provides clear evidence favoring D_U as a better proxy than D_τ and D_η for the effective diffusion coefficient controlling crystal nucleation in stoichiometric oxide glass formers.

Declaration of competing interest

The authors declare that they have no known competing financial interests or personal relationships that could have appeared to influence the work reported in this paper.

Acknowledgments

The authors are grateful to the Brazilian agencies: National Council for Scientific and Technological Development (CNPq), grant numbers 141057/2017-3 (MHRA) and 141816/2018-0 (LRR), and São Paulo Research Foundation (FAPESP), grant no. 2013/07793-6 (CEPID), for the financial support received. This study was financed in part by the Coordenação de Aperfeiçoamento de Pessoal de Nível Superior - Brasil (CAPES) - Finance Code 001.

Appendix A. Supplementary data

Supplementary data to this article can be found online at https://doi.org/10.1016/j.ceramint.2022.01.074.

Appendix

Analysis of the Classical Nucleation Theory in a $BaO{\cdot}2SiO_2$ glass using viscosity and growth velocities as proxies for diffusivity

Using the same approach as for the LS_2 glass, crystal nucleation, growth and viscosity data of $BaO{\cdot}2SiO_2$ (BS_2) were obtained using samples of the *same* glass batch analyzed in Ref. [20]. According to the experimental results presented in Fig. A.1, the new nucleation data for BS_2 at the lowest temperature ($T_n = 943K$) using extended nucleation times (t_n)–up to 36 h–are higher than those presented in Ref. [20] using shorter times (32 h). Additionally, the prediction of the CNT via D_U (dashed curve) led to a T_{max} smaller than that reported in Ref. [20], where the approximation $D \approx D_\eta$ (solid curve) was used. These findings for BS_2 support the more extensive results presented in this work for LS_2 glass. However, this analysis in BS_2 glass requires further studies, using extended t_n at least at two other T_n below the previous T_{max} [20], and a more reliable estimation of N_v by scanning electron microscopy, considering the very high nucleation rate ($I_{max} \sim 10^{12}$ $m^{-3}s^{-1}$) of this glass. Nevertheless, the current results are sufficient to corroborate the conclusions of this work for LS_2.

The small divergence between the $I_{st}(T)$ curves obtained with D_U and D_η even at higher temperatures can be a consequence of the differences in the BS_2 crystal geometry at temperatures above and below T_{max}, going from a spherulitic shape to an irregular one, as shown in the micrographs of Fig. A.2, taken on BS_2 samples heat treated at $T_n = 1053$ (at the top) and 943 K (at the bottom). These factors impair the accurate determination of N_s and crystal sizes, increasing the uncertainty on both I_{st} and $U(T)$.

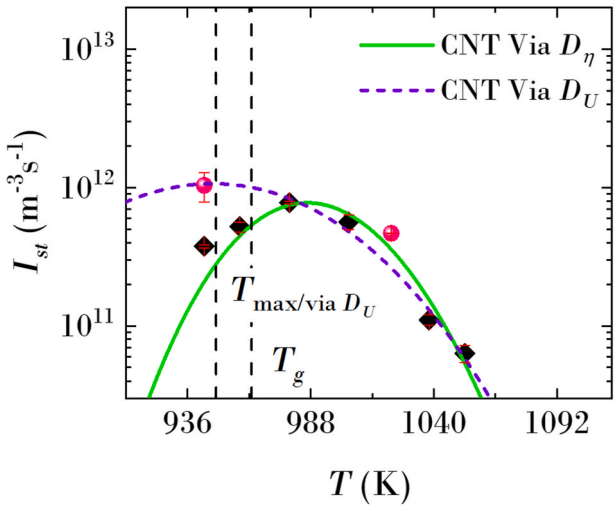

Fig. A.1. Temperature dependence of crystal nucleation rates in the BS_2 system in logarithmic scale. The purple dashed curve and the green solid line denote the CNT prediction using D_U and D_η, respectively, as proxies for diffusivity. The black rhombuses correspond to the data of [20] and the pink dots represent the data of this work using longer treatment times. All properties ($I(T)$, $U(T)$ and $\eta(T)$) were obtained using glass samples of the same batch.

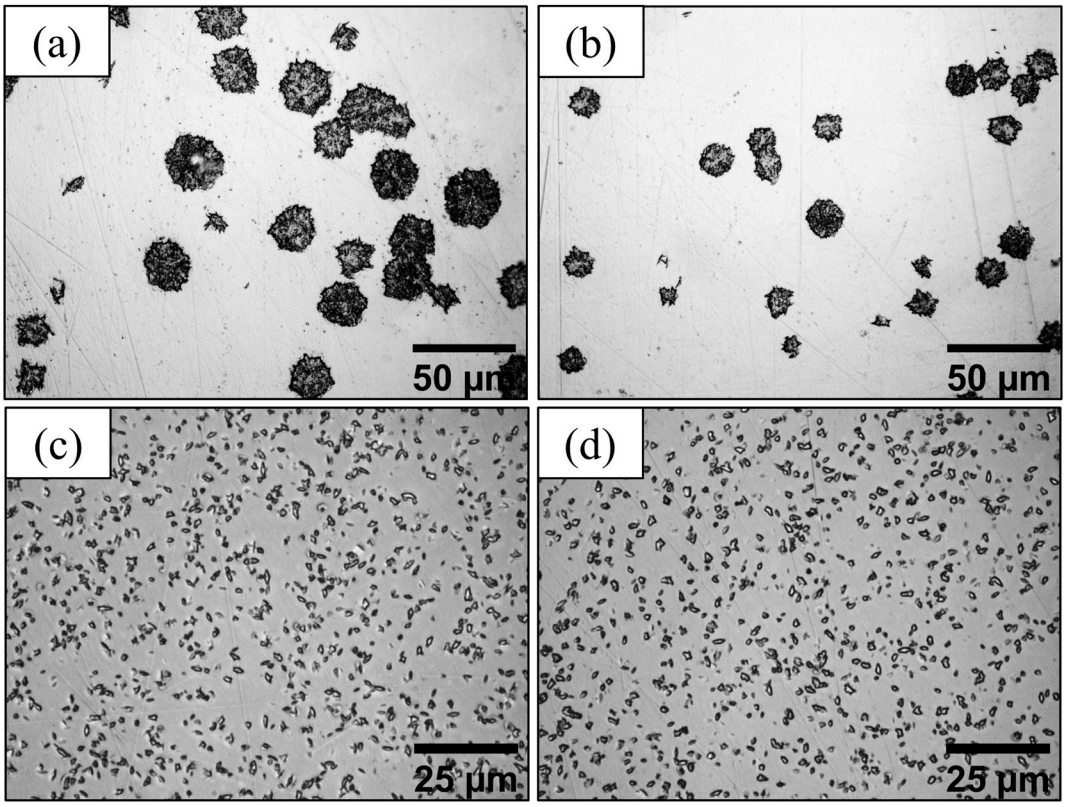

Fig. A.2. Representative optical micrographs of BS_2 samples heat treated at $T_n = 1053\ K$ (at the top) and $T_n = 943\ K$ (at the bottom) for (a) $t_n = 5\ min$, (b) $t_n = 10\ min$, (c) $t_n = 11\ h$, and (d) $t_n = 12\ h$. The same development temperature, $T_d = 1088\ K$, was used in all the cases.

References

[1] V.M. Fokin, J.W.P. Schmelzer, M.L.F. Nascimento, E.D. Zanotto, Diffusion coefficients for crystal nucleation and growth in deeply undercooled glass-forming liquids, J. Chem. Phys. 126 (2007) 234507, https://doi.org/10.1063/1.2746502.

[2] X. Xia, D.C. Van Hoesen, M.E. Mckenzie, R.E. Youngman, O. Gulbiten, K.F. Kelton, Time-dependent nucleation rate measurements in $BaO{\cdot}2SiO_2$ and $5BaO{\cdot}8SiO_2$ glasses, J. Non-Cryst. Solids 525 (2019) 119575, https://doi.org/10.1016/j.jnoncrysol.2019.119575.

[3] J. Deubener, M. Montazerian, S. Krüger, O. Peitl, E.D. Zanotto, Heating rate effects in time-dependent homogeneous nucleation in glasses, J. Non-Cryst. Solids 474 (2017) 1–8, https://doi.org/10.1016/j.jnoncrysol.2017.07.019.

[4] V.M. Fokin, A.S. Abyzov, N.S. Yuritsyn, J.W.P. Schmelzer, E.D. Zanotto, Effect of structural relaxation on crystal nucleation in glasses, Acta Mater. 203 (2021) 9–11, https://doi.org/10.1016/j.actamat.2020.11.014.

[5] J.W.P. Schmelzer, T.V. Tropin, V.M. Fokin, A.S. Abyzov, E.D. Zanotto, Effects of glass transition and structural relaxation on crystal nucleation: theoretical description and model analysis, Entropy 22 (2020) 1–36, https://doi.org/10.3390/e22101098.

[6] L.R. Rodrigues, A.S. Abyzov, V.M. Fokin, E.D. Zanotto, Effect of structural relaxation on crystal nucleation in a soda-lime-silica glass, J. Am. Ceram. Soc. 104 (2021) 3212–3223, https://doi.org/10.1111/jace.17765.

[7] E.D. Zanotto, P.F. James, Experimental tests of the classical nucleation theory for glasses, J. Non-Cryst. Solids 74 (1985) 373–394, https://doi.org/10.1016/0022-3093(85)90080-8.

[8] V.M. Fokin, E.D. Zanotto, N.S. Yuritsyn, J.W.P. Schmelzer, Homogeneous crystal nucleation in silicate glasses: a 40 years perspective, J. Non-Cryst. Solids 352 (2006) 2681–2714, https://doi.org/10.1016/j.jnoncrysol.2006.02.074.

[9] M.L.F. Nascimento, V.M. Fokin, E.D. Zanotto, A.S. Abyzov, Dynamic processes in a silicate liquid from above melting to below the glass transition, J. Chem. Phys. 135 (2011) 194703, https://doi.org/10.1063/1.3656696.

[10] D.C. Van Hoesen, X. Xia, M.E. McKenzie, K.F. Kelton, Modeling nonisothermal crystallization in a $BaO{\bullet}2SiO_2$ glass, J. Am. Ceram. Soc. 103 (2020) 2471–2482, https://doi.org/10.1111/jace.16979.

[11] V.M. Fokin, A.S. Abyzov, A.M. Rodrigues, R.Z. Pompermayer, G.S. Macena, E. D. Zanotto, E.B. Ferreira, Effect of non-stoichiometry on the crystal nucleation and growth in oxide glasses, Acta Mater. 180 (2019) 317–328, https://doi.org/10.1016/j.actamat.2019.09.017.

[12] L. Gránásy, Quantitative analysis of the classical nucleation theory on glass-forming alloys, J. Non-Cryst. Solids 156–158 (1993) 514–518, https://doi.org/10.1016/0022-3093(93)90010-U.

[13] C. Huang, Z. Chen, Y. Gui, C. Shi, G.G.Z. Zhang, L. Yu, Crystal nucleation rates in glass-forming molecular liquids: D-sorbitol, D-arabitol, D-xylitol, and glycerol, J. Chem. Phys. 149 (2018), https://doi.org/10.1063/1.5042112.

[14] V.M. Fokin, M.L.F. Nascimento, E.D. Zanotto, Correlation between maximum crystal growth rate and glass transition temperature of silicate glasses, J. Non-Cryst. Solids 351 (2005) 789–794, https://doi.org/10.1016/j.jnoncrysol.2005.02.005.

[15] A.O. Tipeev, E.D. Zanotto, J.P. Rino, Diffusivity, interfacial free energy, and crystal nucleation in a supercooled Lennard-Jones liquid, J. Phys. Chem. C 122 (2018) 28884–28894, https://doi.org/10.1021/acs.jpcc.8b10637.

[16] S.C.C. Prado, J.P. Rino, E.D. Zanotto, Successful test of the classical nucleation theory by molecular dynamic simulations of BaS, Comput. Mater. Sci. 161 (2019) 99–106, https://doi.org/10.1016/j.commatsci.2019.01.023.

[17] A.O. Tipeev, E.D. Zanotto, J.P. Rino, Crystal nucleation kinetics in supercooled germanium: MD simulations versus experimental data, J. Phys. Chem. B 124 (2020) 7979–7988, https://doi.org/10.1021/acs.jpcb.0c05480.

[18] L. Separdar, J.P. Rino, E.D. Zanotto, Molecular dynamics simulations of spontaneous and seeded nucleation and theoretical calculations for zinc selenide, Comput. Mater. Sci. 187 (2021) 110124, https://doi.org/10.1016/j.commatsci.2020.110124.

[19] V.M. Fokin, A.M. Kalinina, V.N. Filipovich, Nucleation in silicate glasses and effect of preliminary heat treatment on it, J. Cryst. Growth 52 (1981) 115–121, https://doi.org/10.1016/0022-0248(81)90178-0.

[20] M.H.R. Acosta, L.R. Rodrigues, D.R. Cassar, M. Montazerian, O.P. Filho, E. D. Zanotto, Further evidence against the alleged failure of the classical nucleation theory below the glass transition range, J. Am. Ceram. Soc. 104 (2021) 4537–4549, https://doi.org/10.1111/jace.17852.

[21] T. Ogura, R. Hayami, M. Kadota, Kinetics and Mechanism of crystallization of lithium silicate glasses, J. Ceram. Assoc. 76 (1968) 277–284.

[22] C.J.R. Gonzalez-Oliver, P.S. Johnson, P.F. James, Influence of water content on the rates of crystal nucleation and growth in lithia-silica and soda-lime-silica glasses, J. Mater. Sci. 14 (1979) 1159–1169, https://doi.org/10.1007/BF00561300.

[23] J. Deubener, R. Brückner, M. Sternitzke, Induction time analysis of nucleation and crystal growth in di- and metasilicate glasses, J. Non-Cryst. Solids 163 (1993) 1–12, https://doi.org/10.1016/0022-3093(93)90638-E.

[24] L.L. Burgner, M.C. Weinberg, An assessment of crystal growth behavior in lithium disilicate glass, J. Non-Cryst. Solids 279 (2001) 28–43, https://doi.org/10.1016/S0022-3093(00)00325-2.

[25] M.L.F. Nascimento, E. Dutra Zanotto, Does viscosity describe the kinetic barrier for crystal growth from the liquidus to the glass transition? J. Chem. Phys. 133 (2010) 174701, https://doi.org/10.1063/1.3490793.

[26] K. Kelton, A.L. Greer, Nucleation in Condensed Matter: Applications in Materials and Biology, Elsevier, Oxford, 2010.
[27] R.T. DeHoff, F.N. Rhines, Determination of number of particles per unit volume from measurements made on random plane sections: the general cylinder and the ellipsoid, Trans. Met. Soc. AIME. 221 (1961) 975–982.
[28] E.D. Zanotto, P.F. James, A theoretical and experimental assessment of systematic errors in nucleation experiments, J. Non-Cryst. Solids 124 (1990) 86–90, https://doi.org/10.1016/0022-3093(90)91084-5.
[29] D. Kashchiev, Nucleation: Basic Theory with Applications, Elsevier, Oxford, 2000.
[30] J.C. Mauro, Y. Yue, A.J. Ellison, P.K. Gupta, D.C. Allan, Viscosity of glass-forming liquids, Proc. Natl. Acad. Sci. Unit. States Am. 106 (2009) 19780–19784, https://doi.org/10.1073/pnas.0911705106.
[31] K.F. Kelton, Crystal nucleation in liquids and glasses, Solid State Phys. 45 (1991) 75–177.
[32] A.S. Abyzov, V.M. Fokin, N.S. Yuritsyn, A.M. Rodrigues, J.W.P. Schmelzer, The effect of heterogeneous structure of glass-forming liquids on crystal nucleation, J. Non-Cryst. Solids 462 (2017) 32–40, https://doi.org/10.1016/j.jnoncrysol.2017.02.004.
[33] P.K. Gupta, D.R. Cassar, E.D. Zanotto, Role of dynamic heterogeneities in crystal nucleation kinetics in an oxide supercooled liquid, J. Chem. Phys. 145 (2016) 211920, https://doi.org/10.1063/1.4964674.
[34] V.M. Fokin, R.M.C.V. Reis, A.S. Abyzov, C.R. Chinaglia, E.D. Zanotto, Nonstoichiometric crystallization of lithium metasilicate – calcium metasilicate glasses. Part 1 — crystal nucleation and growth rates, J. Non-Cryst. Solids 362 (2013) 56–64, https://doi.org/10.1016/j.jnoncrysol.2012.11.020.
[35] K. Takahashi, T. Yoshio, Thermodynamic quantities of alkali silicates in the temperature range from 25 C to melting point, J. Ceram. Soc. Jpn. 81 (1973) 524.
[36] A. Einstein, On the motion of small particles suspended in liquids at rest required by the molecular-kinetic theory of heat, Ann. Phys. 17 (1905) 549–560.
[37] H. Eyring, Viscosity, plasticity, and diffusion as examples of absolute reaction rates, J. Chem. Phys. 4 (1936) 283–291, https://doi.org/10.1063/1.1749836.
[38] A.A. Cabral, V.M. Fokin, E.D. Zanotto, Nanocrystallization of fresnoite glass. II. Analysis of homogeneous nucleation kinetics, J. Non-Cryst. Solids 343 (2004) 85–90, https://doi.org/10.1016/j.jnoncrysol.2004.06.020.
[39] K.F. Kelton, A.L. Greer, Nucleation in Condensed Matter: Applications in Materials and Biology, Elsevier, Oxford, 2010.
[40] D.R. Cassar, Solving the classical nucleation theory with respect to the surface energy, J. Non-Cryst. Solids 511 (2019) 183–185, https://doi.org/10.1016/j.jnoncrysol.2019.02.006.
[41] E.O. Lebigot, Uncertainties: a Python package for calculations with uncertainties, (n.d.). http://pythonhosted.org/uncertainties/(accessed March 27, 2014).
[42] A.M. Rodrigues, D.R. Cassar, V.M. Fokin, E.D. Zanotto, Crystal growth and viscous flow in barium disilicate glass, J. Non-Cryst. Solids 479 (2018) 55–61, https://doi.org/10.1016/j.jnoncrysol.2017.10.007.
[43] X. Xia, D.C. Van Hoesen, M.E. Mckenzie, R.E. Youngman, K.F. Kelton, Low-temperature nucleation anomaly in silicate glasses shown to be artifact in a $5BaO{\cdot}8SiO_2$ glass, Nat. Commun. 12 (2021) 1–6, https://doi.org/10.1038/s41467-021-22161-9, 2026.
[44] S. Buchner, A.S. Pereira, J.C. de Lima, N.M. Balzaretti, Effect of annealing close to Tg on the short-range order of lithium disilicate glass, J. Non-Cryst. Solids 560 (2021) 120729, https://doi.org/10.1016/j.jnoncrysol.2021.120729.
[45] S. An, Y. Li, J. Li, S. Zhao, B. Liu, P. Guan, The linear relationship between diffusivity and crystallization kinetics in a deeply supercooled liquid $Ni_{50}Ti_{50}$ alloy, Acta Mater. 152 (2018) 1–6, https://doi.org/10.1016/j.actamat.2018.04.008.